Journal Pre-proof

Nanostructured multiferroic $Pb(Zr,Ti)O_3$–$NiFe_2O_4$ thin-film composites

Aleksander Matavž, Primož Koželj, Maximilian Winkler, Korbinian Geirhos, Peter Lunkenheimer, Vid Bobnar

PII: S0040-6090(21)00223-6
DOI: https://doi.org/10.1016/j.tsf.2021.138740
Reference: TSF 138740

To appear in: *Thin Solid Films*

Received date: 27 November 2020
Revised date: 27 April 2021
Accepted date: 6 May 2021

Please cite this article as: Aleksander Matavž, Primož Koželj, Maximilian Winkler, Korbinian Geirhos, Peter Lunkenheimer, Vid Bobnar, Nanostructured multiferroic $Pb(Zr,Ti)O_3$–$NiFe_2O_4$ thin-film composites, *Thin Solid Films* (2021), doi: https://doi.org/10.1016/j.tsf.2021.138740

- $NiFe_2O_4$ embedded into self-assembled highly-porous $Pb(Zr,Ti)O_3$ thin films.
- Pure two phase ferromagnetic–ferroelectric thin-film composites.
- Direct stress coupling between magnetostrictive and piezoelectric grains.
- Multiferroic and magnetocapacitive response of films.

Nanostructured multiferroic $Pb(Zr,Ti)O_3$–$NiFe_2O_4$ thin-film composites

Aleksander Matavž,[a,1], Primož Koželj,[a,c,2], Maximilian Winkler[d], Korbinian Geirhos[d], Peter Lunkenheimer[d], Vid Bobnar[a,b,*]

[a] *Jožef Stefan Institute, Jamova cesta 39, SI-1000 Ljubljana, Slovenia*
[b] *Jožef Stefan International Postgraduate School, Jamova cesta 39, SI-1000 Ljubljana, Slovenia*
[c] *Faculty of Mathematics and Physics, University of Ljubljana, Jadranska 19, SI-1000 Ljubljana, Slovenia*
[d] *Experimental Physics V, Center for Electronic Correlations and Magnetism, University of Augsburg, 86159 Augsburg, Germany*

Abstract

$Pb(Zr,Ti)O_3$–$NiFe_2O_4$ thin-film composites were fabricated by spin coating a nickel ferrite precursor solution onto self-assembled porous lead zirconate titanate thin films. The morphology investigations revealed a very extensive interface area between both constitutents. The X-ray diffraction shows that $NiFe_2O_4$ coatings induce large compressive in-plane stresses in $Pb(Zr,Ti)O_3$, which are generated during synthesis due to the significant difference in the thermal expansion coefficients of both phases. Diffraction peaks, moreover, corroborate a two phase pure system, without any other detectable secondary phase. The multiferroicity of the composites is evidenced by both ferroelectric and ferromagnetic hysteresis loops, while magnetic field-induced changes of the dielectric constant imply the potential utility of the developed material in magnetocapacitive applications.

Keywords: Lead zirconate titanate, Nickel ferrite, Nanostructured films, Thin-film composites, Multiferroics, Magnetoelectrics

1. Introduction

The term multiferroics refers to materials that simultaneously display at least two ferroic properties, (anti)ferromagnetism, (anti)ferroelectricity, ferroelasticity, or ferrotoroidicity [1]. Their renewed interest is due to the fact that if these ferroic orders were coupled new functionalities would emerge. Nowadays, the term is usually used to describe the magnetoelectric multiferroics that are simultaneously ferromagnetic and ferroelectric, with existing cross-coupling between the ferroic order parameters [2, 3] which gives them

*Corresponding author. *Tel.:* +386 1 477 3172, *Fax:* +386 1 251 9385
Email address: vid.bobnar@ijs.si (Vid Bobnar)
[1] currently at cMACS, KU Leuven, Belgium
[2] currently at Max Planck Institute for Chemical Physics of Solids, Dresden, Germany

a tremendous application potential in functional devices in the fields of sensors, data storage, and energy harvesters [4, 5, 6]. However, single-phase multiferroic materials displaying ferroelectricity and ferromagnetism at room temperature are very rare, and their magnetoelectric coupling is typically very weak, which limits their use in practical devices [7, 8]. The synthesis of multiferroic composite materials thus arises as an alternative method for simultaneously obtaining ferroelectric and ferromagnetic properties as well as a higher degree of magnetoelectric coupling [9].

Compared to bulk composites, thin-films exhibit unique advantages: their composition and connectivity can be modulated at the microscopic scale, which eventually leads to the artificial heterostructures with huge application potential. Composites of spinel ferrites Ni(Co,Mn)Fe_2O_4 and ferroelectric ceramics such as $BaTiO_3$ or Pb(Zr,Ti)O_3 have up to now been prepared as bulk sintered ceramics [10] or in thin-film configuration, either as bi- [11] or multi-layers [12] or, alternatively, as thin-film composites prepared by sol-gel [13], pulsed laser deposition [14], and radio frequency (RF) sputtering techniques [15]. In these multiferroic composites the magnetoelectric effect arises from direct stress coupling between magnetostrictive (ferromagnetic) and piezoelectric (ferroelectric) grains – the magnetostrictive layer is deformed under an applied magnetic field and this strain/stress is transferred onto the piezoelectric material that generates voltage due to the direct piezoelectric effect. It is thus evident that good and extensive connectivity among the constituents might result in significant coupling between the piezoelectric and magnetostrictive phases and enhance the magnetoelectric effects.

We present multiferroic thin-film composites with a morphology that provides such an extensive connectivity between the magnetostrictive and piezoelectric constituents. They were fabricated by embedding ferromagnetic $NiFe_2O_4$ into self-assembled highly-porous ferroelectric Pb(Zr,Ti)O_3 thin films. The developed two phase system exhibitis both ferroelectric and ferromagnetic behavior, while measurable magnetic field–induced changes of the dielectric response indicate a direct stress coupling between the magnetostrictive $NiFe_2O_4$ and piezoelectric Pb(Zr,Ti)O_3 grains.

2. Materials and methods

Highly–porous $Pb(Zr_{0.53}Ti_{0.47})O_3$ (denoted as PZT in the following text) films were synthesized on Pt(111)/TiO_2/SiO_2/Si wafers (SINTEF, 625 μm thick) by utilizing an in-house-developed soft-chemistry technique based on the self-assembly of organometallic precursors in a polymer matrix. The focal points of this chemical solution deposition method are: (i) polyvinylpyrrolidone (PVP) is added to the sol-gel precursor solution, composed of organometallic precursors and solvent, to yield a stable and viscous coating solution,

(ii) upon spin coating the exposure to the air humidity initiates the hydrolysis and condensation reactions of the sol-gel precursors and leads to phase separation mediated by PVP molecules, (iii) a subsequent high-temperature treatment causes the organic phase to decompose and induces the crystallization and sintering of the nearby particles. The coating solution used to synthesize porous PZT films consisted of 1 M solution of PZT precursors and 0.5 M solution of PVP. The solution was spin-coated at 3000 rpm for 30 s. Immediately after coating the films were placed on hot plates pre-heated at 150 °C for 2 min and at 350 °C for 5 min and afterwards crystallized at 800 °C for 5 min in a rapid thermal annealing furnace (Mila-500, ULVAC). The whole procedure is precisely described in Ref. [16], where also structural and functional properties of the developed about 1 μm thick films are reported in detail.

$NiFe_2O_4$ (NFO) precursor solution (0.5 M concentration) was prepared by dissolution of iron nitrate hexahydrate and zinc acetate hydrate in 2-methoxyethanol. The solution was heated to 60 °C and stirred for 1 h. The exact amount of bound water in starting chemicals was checked by thermogravity. PZT-NFO composite thin films were prepared by spin coating the NFO precursor solution onto porous PZT films at 3000 rpm for 30 s. The samples were heated on hot plates set at 150 °C and 350 °C for 2 min each, and crystallized at 750 °C for 1 min in a rapid thermal annealing furnace. In order to increase the amount of embedded NFO the whole procedure was repeated 3, 6, or 9 times.

The morphology of the composites was investigated using a JEOL JSM-7600F Field-Emission Scanning Electron Microscope (FE-SEM) with accelerating voltage of 5 kV. X-ray diffraction (XRD) patterns were obtained with a Panalytical X'Pert Pro X-ray diffractometer in the Gonio mode, using Cu-Kα_1 radiation. In order to avoid detector saturation due to a very strong Pt(111) peak, XRD patterns were collected over the 10°-39.3° and 40.7°-60° angular ranges. Magnetic characterization was performed employing a superconducting quantum interference device (MPMS3, Quantum Design). The sample (5 mm × 4 mm) was coated and attached to a quartz paddle sample holder with insulating varnish (GE Varnish, CMR-Direct). The magnetic field was applied in the plane of the film and the magnetic moment of the substrate was subtracted from the measured results. A pure Pd reference sample was measured with the same hysteresis loop measurement sequence, so that the magnetic field offset caused by the remananence of the magnetometer's superconducting magnet could be compensated for.

For dielectric characterization, the remaining pores in the films were filled with epoxy resin (Microchem SU-8 3010, diluted to 40 w/w%) by spin coating. The epoxy was cured at 90 °C and cross-linked under ultraviolet illumination (LS0212 lamp, Lot Oriel Gruppe) before hard-baking at 150 °C and 250 °C. About 100 nm thick Au top electrodes were deposited through shadow masks (diameter of 0.4 mm) by RF-sputtering

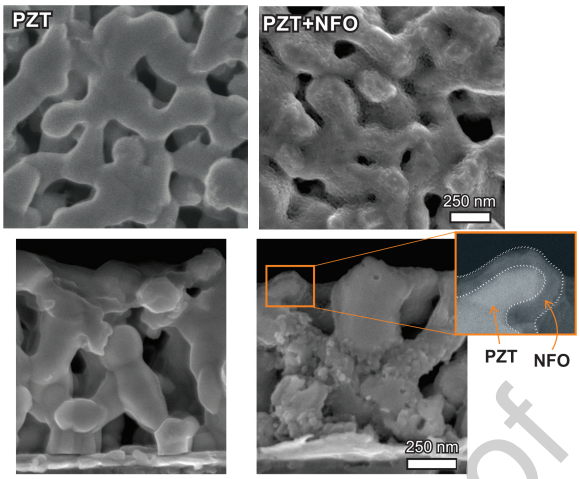

Figure 1: Secondary electron SEM images of the porous PZT film and PZT-NFO composite film (9 NFO layers). The film surfaces are shown in the top row and their cross section in the bottom row. The bottom right inset shows the overlay image of secondary electron and backscattered electron images, which is used to enhance the contrast between PZT and NFO phases.

(Auto 306, 5Pascal). The epoxy resin was then burned out by heating the samples to 450 °C with a heating rate of 50 °C/min. The electrodes were connected to aixACCT TF2000FE ferroelectric test unit by needle-type micromanipulators, and the polarization vs. electric field (P–E) loops were measured with a triangular test signal having a frequency of 100 Hz. For the magnetocapacitive measurements, the sample was inserted into a physical property measurement system from Quantum Design using a special holder, with the magnetic field perpendicular to the film plane. Here, the resin was left in the pores and the samples were polished prior to application of top electrodes, to which the wires were attached by using a silver conductive paint. The temperature dependent dielectric response in different magnetic fields was then measured by a Keysight E4980A Precision LCR Meter, using sinusoidal test signals of various frequencies and with an amplitude of 100 mV. The values of the real part of the dielectric constant, i.e., the dielectric permittivity ε', and the values of the real part of the electrical conductivity, σ', were calculated from the actual measured quantities, capacitance C and electrical conductance G via $\varepsilon' = Cd/\varepsilon_0 S$ and $\sigma' = Gd/S$, where d is the sample thickness, S is the electrode area, and $\varepsilon_0 = 8.85 \times 10^{-12}$ As/Vm is the permittivity of free space.

3. Results and discussion

The morphology of porous PZT films and PZT-NFO thin-film composites is revealed by SEM images of the film surfaces and their cross sections in Figure 1. Even after deposition of 9 NFO layers (bottom right inset), a sponge-like PZT structure is only wrapped by NFO, while samples retain a high level of

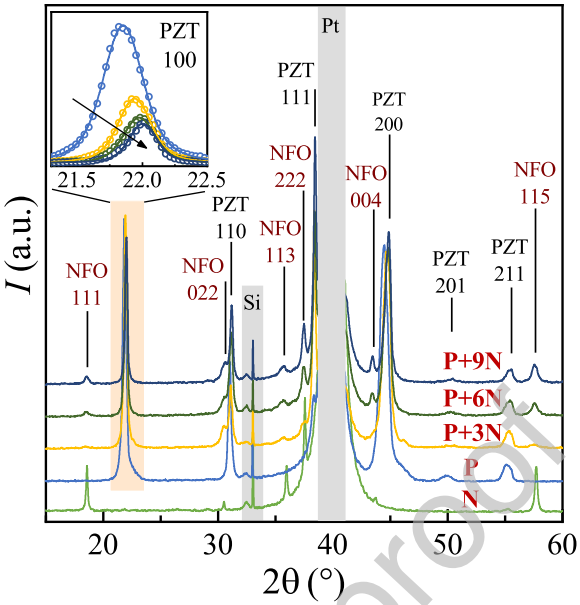

Figure 2: X-ray diffraction patterns of the pure NFO film (N), porous PZT film (P), and PZT-NFO thin-film composites (P-N) with 3, 6, and 9 deposited NFO layers (from bottom to top). The peaks due to the substrate are shaded in gray. The inset highlights the shift in the PZT 100 peak position towards higher 2Θ values with increasing number of NFO layers (indicated by an arrow). The solid lines through the experimental points are fits to the Voigt profile function.

porosity. Due to this unique samples' geometrical feature, a very extensive interface area exists between both constitutents, and since the thermal expansion coefficients of NFO ($\alpha = 12.9 \times 10^{-6}$ K^{-1}) [17] and PZT ($\alpha = 5.5 \times 10^{-6}$ K^{-1}) [18] are significantly different, large thermal residual stresses are generated during synthesis.

The compressive residual stresses, introduced in the $Pb(Zr,Ti)O_3$, are clearly evidenced by a systematical shift (distinctly depicted in the inset to Figure 2) in the PZT 100 X-ray diffraction peak position towards higher 2Θ values with increasing number of NFO layers. The solid lines through the experimental points are fits to the Voigt profile function, while the intensity of the peaks decreases due to higher absorption of the PZT-scattered X-rays in the progressively thicker NFO layer. The main frame of Figure 2 presents XRD patterns of the pure NFO film (N), porous PZT film (P), and PZT-NFO thin-film composites (P-N) with different number of deposited NFO layers. The diffraction peaks corroborate a two phase system without any other detectable secondary phase and thus indicate that PZT and NFO are compatible at the firing temperatures – there is no chemical reaction and no solid solubility between both constituents. The comparison of XRD peak intensities reveal slight 100 texture of PZT and 111 texture of NFO phase.

The multiferroicity of the developed PZT-NFO thin-film composites is evidenced in Figure 3, which

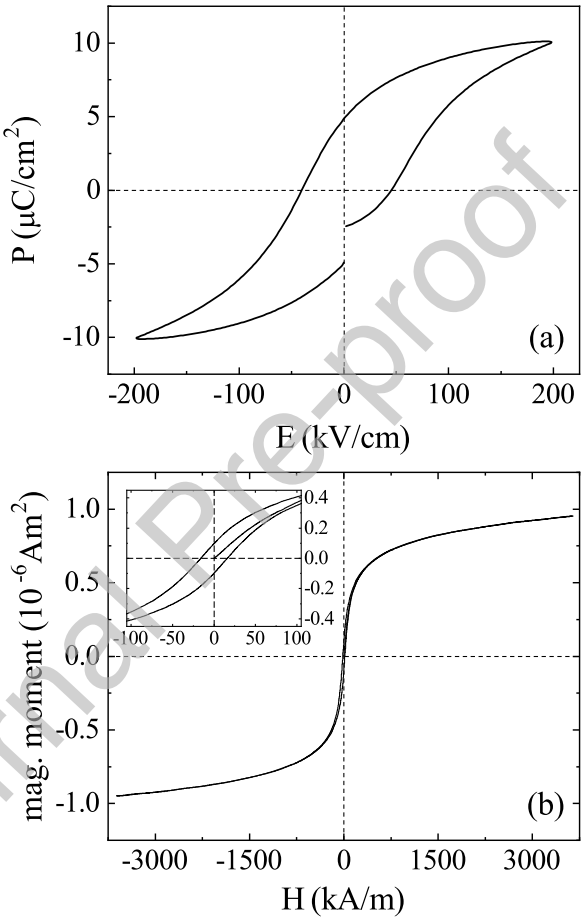

Figure 3: Multiferroic response of PZT-NFO thin-film composites: (a) Polarization vs. electric field and (b) magnetic moment vs. magnetic field hysteresis loops. The inset in (b) shows a zoom of the ferromagnetic hysteresis loop at low magnetic fields.

depicts both, ferroelectric and ferromagnetic hysteresis loops. A single ferroelectric P–E hysteresis loop was detected shortly after a preceding prepolarization pulse – thus the difference between starting ($P = -2.47$ μC/cm^2) and ending ($P = -4.90$ μC/cm^2) polarization values provides also the information on the level of sample's depolarization within the time period of 1 s between the prepolarization and measurement pulses. The value of remanent polarization $P_r = 4.90$ μC/cm^2 is significantly lower than values detected in the pure porous PZT films [16]. The difference could be due to (i) depolarizing effects of NFO layer and (ii) changes in domain structure in PZT due to residual stresses. The depolarizing effects appear due to the presence of NFO layer that covers the PZT phase. NFO has low dielectric permittivity and acts as dead layer; hence, the NFO layer will cause a tilt of a square-shaped P-E loops of pure PZT and lead to lower P_r values [19]. On the other hand, the residual thermal stress in combination with mechanical constraint of the electromechanically inactive NFO layer will have similar effects on the ferroelectric behavior of composites [20]. The results also clearly display hysteretic magnetic behavior with a typical coercitivity of ≈16 kA/m (Figure 3b).

It has been postulated that the magnetoelectric effect in composites of PZT and spinel ferrites comes from a direct stress coupling between magnetostrictive $NiFe_2O_4$ or $CoFe_2O_4$ and piezoelectric PZT grains [13, 14, 15]. Since the morphology of our thin-film composites provides a very extensive connectivity among the constituents, a significant coupling between the piezoelectric and magnetostrictive phases might exist. The main frames of Figure 4 present the dielectric response, measured at various frequencies over a broad temperature range in three different magnetic fields. At first glance, the results seem to be independent of magnetic field, however, precise measurements of the magnetocapacitive response MC=[$\varepsilon'(H)$-$\varepsilon'(H{=}0)$]/$\varepsilon'(H{=}0)$ reveal slight magnetic field–induced changes of the dielectric response, as treated in the next paragraph. The general behavior of $\varepsilon'(T)$ in Figure 4 reminds of a relaxational process, which we assume to be of non-intrinsic Maxwell-Wagner (MW) type. MW relaxations can arise from depletion layers at the interface between sample and contacts, grain boundaries, or simply by the heterogeneous nature of the present two-component material [21, 22]. The conductivity $\sigma'(T)$ shown in the lower frame of Figure 4, which is proportional to the dielectric loss ε'', seems to be dominated by dc and ac charge-transport processes arising from hopping conductivity, whose detailed treatment, however, is out of the scope of the present work.

The inset to Figure 4 presents the MC data, detected at constant temperature of 300 K on a polarized sample (i.e., a dc electric field of 200 kV/cm was applied for 10 min well before the measurement). It should be stressed that the results obtained at a frequency of 190 Hz do not unequivocally confirm the

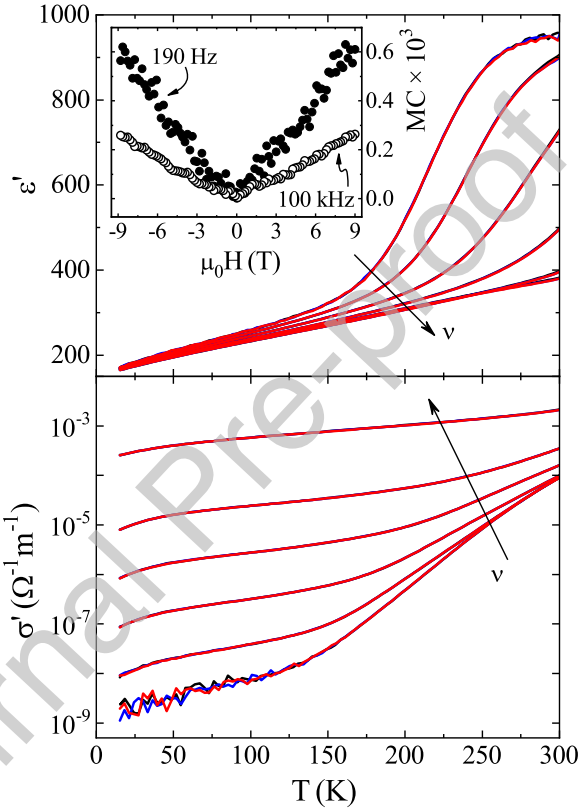

Figure 4: Real parts of the dielectric constant, ε', and electrical conductivity, σ', measured at various frequencies (20 Hz, 121 Hz, 1.16 kHz, 11.1 kHz, 100 kHz, 1MHz) over broad temperature range in three different magnetic fields (0, 4.5 T, 9 T, presented in black, blue, and red, respectively). The inset shows the magnetocapacitive response MC=[$\varepsilon'(H)$-$\varepsilon'(H$=0)]/$\varepsilon'(H$=0) of a polarized sample, detected at 300 K at two different frequencies of 190 Hz and 100 kHz.

magnetoelectric coupling between PZT and NFO. Namely, the observed strong frequency dependence of ε' values at low frequencies in the main frame is due to the (i) sample's ac conductivity [23] and/or (ii) MW-type contributions, which are often found in multiferroic thin films [15, 24, 25] – and it has been argued that magnetoresistive samples with MW behavior might display magnetocapacitance, which cannot be taken as an evidence of magnetoelectric coupling [26, 27]. On the other hand, the MC data, detected at a frequency of 100 kHz, which is well beyond the frequency range where MW behavior plays a role (ε' is almost independent of frequency above 100 kHz, see the main frame), indicate a direct stress coupling between both components of the film.

4. Summary

Multiferroic thin-film composites were developed by embedding ferromagnetic $NiFe_2O_4$ into self-assembled porous ferroelectric $Pb(Zr,Ti)O_3$ thin films. Although bi- or multi-layers of spinel ferrites and $Pb(Zr,Ti)O_3$ have already been fabricated, or, alternatively, their composites were prepared by sol-gel or RF sputtering techniques [11, 12, 13, 14, 15], the morphology of our system provides a very extensive connectivity between the magnetostrictive and piezoelectric constituents. Detailed structural (SEM, XRD) investigations revealed a pure two-phase system, without any chemical reaction or solid solubility between both constituents during synthesis. The multiferroicity of composites was evidenced by detecting both ferroelectric and ferromagnetic hysteresis loops. A measurable magnetic field–induced changes of the dielectric constant, not only at low frequencies but also above the characteristic frequencies of the Maxwell-Wagner behavior, indicate a direct stress coupling between the magnetostrictive $NiFe_2O_4$ and piezoelectric $Pb(Zr,Ti)O_3$ grains and imply the potential utility of the developed material in magnetocapacitive applications.

Acknowledgements

This research was supported by the Slovenian Research Agency under program P1-0125 and project J2-1740 and by the Deutsche Forschungsgemeinschaft through the Transregional Collaborative Research Center TRR 80.

References

[1] C. Lu, M. Wu, L. Lin, J.-M. Liu, Single-phase multiferroics: new materials, phenomena, and physics, Natl. Sci. Rev. 6 (2019) 653-668, https://doi.org/10.1093/nsr/nwz091.

[2] W. Eerenstein, N.D. Mathur, J.F. Scott, Multiferroic and magnetoelectric materials, Nature 442 (2006) 759-765, https://doi.org/10.1038/nature05023.

[3] R. Ramesh, N.A. Spaldin, Multiferroics: progress and prospects in thin films, Nat. Mater. 6 (2007) 21-29, https://doi.org/10.1038/nmat1805.

[4] J.F. Scott, Multiferroic memories, Nat. Mater. 6 (2007) 256-257, https://doi.org/10.1038/nmat1868.

[5] C.M. Leung, J. Li, D. Viehland, X. Zhuang, A review on applications of magnetoelectric composites: from heterostructural uncooled magnetic sensors, energy harvesters to highly efficient power converters, J. Phys. D. Appl. Phys. 51 (2018) 263002, http://dx.doi.org/10.1088/1361-6463/aac60b.

[6] F. Narita, M. Fox, A review on piezoelectric, magnetostrictive, and magnetoelectric materials and device technologies for energy harvesting applications, Adv. Eng. Mater. 20 (2018) 1700743, http://dx.doi.org/10.1002/adem.201700743.

[7] N.A. Hill, Why are there so few magnetic ferroelectrics?, J. Phys. Chem. B 104 (2000) 6694-6709, https://doi.org/10.1021/jp000114x.

[8] W. Prellier, M.P. Singh, P. Murugavel, The single-phase multiferroic oxides: from bulk to thin film, J. Phys. Condens. Matter. 17 (2005) R803-R832, http://dx.doi.org/10.1088/0953-8984/17/30/R01.

[9] C.W. Nan, M.I. Bichurin, S. Dong, D. Viehland, G. Srinivasan, Multiferroic magnetoelectric composites: historical perspective, status, and future directions, J. Appl. Phys. 103 (2008) 031101, http://dx.doi.org/10.1063/1.2836410.

[10] K. Srinivas, G. Prasad, T. Bhimasankaram, S.V. Suryanarayana, Electromechanical coefficients of magnetoelectric PZT–$CoFe_2O_4$ composite, Mod. Phys. Lett. B 14 (2000) 663-674, https://doi.org/10.1142/S021798490000080X.

[11] X.D. Zhang, J. Dho, Electric and magnetic properties of a $CoFe_2O_4$/PZT bilayer grown on (100)$SrTiO_3$ by using PLD, J. Korean Phys. Soc. 56 (2010) 383-387, https://doi.org/10.3938/jkps.56.383.

[12] L. Jian, A.S. Kumar, C.S.C. Lekha, S. Vivek, I. Salvado, A.L. Kholkin, S.S. Nair, Strong sub-resonance magnetoelectric coupling in PZT-$NiFe_2O_4$-PZT thin film composite, Nano-Structures & Nano-Objects 18 (2019) 100272, https://doi.org/10.1016/j.nanoso.2019.100272.

[13] J.G. Wana, X.W. Wang, Y.J. Wu, M. Zeng, Y. Wang, H. Jiang, W.Q. Zhou, G.H. Wang, J.-M. Liu, Magnetoelectric $CoFe_2O_4$–Pb(Zr,Ti)O_3 composite thin films derived by a sol-gel process, Appl. Phys. Lett. 86 (2005) 122501, https://doi.org/10.1063/1.1889237.

[14] H. Ryu, P. Murugavel, J.H. Lee, S.C. Chae, T.W. Noh, Magnetoelectric effects of nanoparticulate $Pb(Zr_{0.52}Ti_{0.48})O_3$–$NiFe_2O_4$ composite films, Appl. Phys. Lett. 89 (2006) 102907, https://doi.org/10.1063/1.2338766.

[15] I. Fina, N. Dix, L. Fàbrega, F. Sánchez, J. Fontcuberta, Magnetocapacitance in $BaTiO_3$–$CoFe_2O_4$ nanocomposites, Thin Solid Films 518 (2010) 4634-4636, https://doi.org/10.1016/j.tsf.2009.12.048.

[16] A. Matavž, A. Bradeško, T. Rojac, B. Malič, V. Bobnar, Self-assembled porous ferroelectric thin films with a greatly enhanced piezoelectric response, Appl. Mater. Today 16 (2019) 83-89, https://doi.org/10.1016/j.apmt.2019.04.008.

[17] A.T. Nelson, J.T. White, D.A. Andersson, J.A. Aguiar, K.J. McClellan, D.D. Byler, M.P. Short, C.R. Stanek, Thermal expansion, heat capacity, and thermal conductivity of nickel ferrite ($NiFe_2O_4$), J. Am. Ceram. Soc. 97 (2014) 1559-1565, https://doi.org/10.1111/jace.12901.

[18] G. Han, J. Ryu, W.-H. Yoon, J.-J. Choi, B.-D. Hahn, J.-W. Kim, D.-S. Park, C.-W. Ahn, S. Priya, D.-Y. Jeong, Stress-controlled $Pb(Zr_{0.52}Ti_{0.48})O_3$ thick films by thermal expansion mismatch between substrate and $Pb(Zr_{0.52}Ti_{0.48})O_3$ film, J. Appl. Phys. 110 (2011) 124101, https://doi.org/10.1063/1.3669384.

[19] U. Böttger, R. Waser, Interaction between depolarization effects, interface layer, and fatigue behavior in PZT thin film

capacitors, J. Appl. Phys. 122 (2017) 024105, https://doi.org/10.1063/1.4992812.

[20] K. Coleman, J. Walker, T. Beechem, S. Trolier-McKinstry, Effect of stresses on the dielectric and piezoelectric properties of $Pb(Zr_{0.52}Ti_{0.48})O_3$ thin films, J. Appl. Phys. 126 (2019) 034101, https://doi.org/10.1063/1.5095765.

[21] A.R. von Hippel, *Dielectrics and Waves* (John Wiley & Sons, New York, 1954).

[22] P. Lunkenheimer, V. Bobnar, A.V. Pronin, A.I. Ritus, A.A. Volkov, A. Loidl, Origin of apparent colossal dielectric constants, Phys. Rev. B 66 (2002) 052105, https://doi.org/10.1103/PhysRevB.66.052105.

[23] A.K. Jonscher, *Dielectric Relaxations in Solids* (Chelsea Dielectrics Press, London, 1983).

[24] N. Ortega, P. Bhattacharya, R.S. Katiyar, P. Dutta, A. Manivannan, M.S. Seehra, I. Takeuchi, S.B. Majumder, Multiferroic properties of $Pb(Zr,Ti)O_3$–$CoFe_2O_4$ composite thin films, J. Appl. Phys. 100 (2006) 126105, https://doi.org/10.1063/1.2400795.

[25] R. Schmidt, W. Eerenstein, T. Winiecki, F.D. Morrison, P.A. Midgley, Impedance spectroscopy of epitaxial multiferroic thin films, Phys. Rev. B 75 (2007) 245111, https://doi.org/10.1103/PhysRevB.75.245111.

[26] G. Catalan, Magnetocapacitance without magnetoelectric coupling, Appl. Phys. Lett. 88 (2006) 102902, https://doi.org/10.1063/1.2177543.

[27] H.M. Jang, J.H. Park, S. Ryu, S.R. Shannigrahi, Magnetoelectric coupling susceptibility from magnetodielectric effect, Appl. Phys. Lett. 93 (2008) 252904, https://doi.org/10.1063/1.3050533.

Declaration of interests

☒ The authors declare that they have no known competing financial interests or personal relationships that could have appeared to influence the work reported in this paper.

☐The authors declare the following financial interests/personal relationships which may be considered as potential competing interests:

Aleksander Matavž: Conceptualization, Investigation, Writing
Primož Koželj: Investigation
Maximilian Winkler: Investigation
Korbinian Geirhos: Investigation
Peter Lunkenheimer: Investigation, Supervision, Funding acquisition
Vid Bobnar: Conceptualization, Writing, Supervision, Funding acquisition